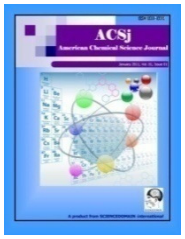

*American Chemical Science Journal*
*4(5): 554-575, 2014*

**SCIENCEDOMAIN** *international*
www.sciencedomain.org

# A Quantum-Chemical Study of the *In vitro* Cytotoxicity of a Series of (*Z*)-1-Aryl-3-Arylamino-2-Propen-1-Ones Against Human Tumor DU145 and K562 Cell Lines

**Diego I. Pino-Ramírez[1] and Juan S. Gómez-Jeria[1*]**

*[1]Quantum Pharmacology Unit, Department of Chemistry, Faculty of Sciences, University of Chile. Las Palmeras 3425, Nuñoa, Santiago 7800003, Santiago, Chile.*

***Authors' contributions***

*This work was carried out in collaboration between both authors. Both authors read and approved the final manuscript.*

***Original Research Article***

***Received 26th December 2013***
***Accepted 13th February 2014***
***Published 31st March 2014***

## ABSTRACT

In this paper we present the results of a formal quantum-chemical analysis of the relationships between the electronic structure and *In vitro* cytotoxicity activity (measured in a cell-based assay using two different human tumor cell lines derived from human prostate cancer and leukemia) for a series of (*Z*)-1-aryl-3-arylamino-2-propen-1-ones. We employed a formal method relating biological activities with local atomic reactivity indices developed in our Unit. The electronic structure of all molecules was calculated within Density Functional Theory at the B3LYP/6-31g (d,p) level of theory with full geometry optimization. We have obtained statistically significant results relating the variation of a definite set of local atomic reactivity indices to the variation of toxicity against the DU-145 cell line. No local atomic reactivity indices belonging to the chain joining the phenyl rings appear in the final equation. Therefore it is not possible to elaborate about its role. Phenyl rings seem to play opposite roles regarding electron transfer. The whole process is charge-, orbital- and sterically-controlled. No good results were obtained for the K562 cell line. More experimental information is needed to clarify this last result.

**Corresponding author: Email: facien03@uchile.cl;*

*Keywords:* (*Z*)-1-aryl-3-arylamino-2-propen-1-ones*; QSAR, local atomic reactivity indices; cytotoxicity; Quantum Chemistry; SAR; antiproliferative action; DU-145 cell line; K562 cell line; leukemia; human prostate cancer.*

## 1. INTRODUCTION

Microtubules (MTs) are components of the cytoskeleton composed of α- and β-tubulin forming heterodimers [1-4]. MTs play a vital role in numerous essential cellular functions, such as cell transport, cell movement, the preservation of cellular morphology, cell division and cell signaling. In the eukaryotic cell cycle tubulin is polymerized into MTs, which form the mitotic spindle. The spindle then moves the chromosomes to the opposite sides of the cell, in preparation for cell division into two daughter cells. Tubulin polymerization and depolymerization are very dynamic processes which are tightly regulated. Any interference with these processes can cause cell cycle arrest in the mitotic phase and ensuing cell apoptosis. Because of this central role in cell proliferation, MTs have been recognized as successful and effective targets for the development of novel anti-cancer drugs [5-10]. Anti-microtubule agents can be classified into two classes following their action: microtubule-stabilizing agents (paclitaxel and docetaxel for example), and inhibitors of tubulin polymerization (such as combretastatin, vincristine, vinblastine, and colchicines).

An improved knowledge about the microscopic action mechanisms through which synthetic ligands exert their effect(s) on MTs is of paramount importance for designing new and more powerful drugs [8,9,11-30]. Several families of molecules which inhibit tubulin polymerization have been reported in the literature. On the other hand, few reports have described small man-made molecules that stimulate tubulin polymerization and microtubule stabilization. Recently, Reddy et al. synthesized a series of (*Z*)-1-aryl-3-arylamino-2-propen-1-ones and evaluated them for their antiproliferative activity in a cell-based assay using two different human tumor cell lines derived from human prostate cancer (DU145) and leukemia (K562) [21]. These molecules seem to represent a new class of microtubule-stabilizing agents. In this paper we present the results of a formal quantum-chemical analysis of the relationships between the electronic structure and *In vitro* cytotoxicity of the abovementioned molecules.

## 2. MODELS, METHODS AND CALCULATIONS

### 2.1 Model

In the following we shall present the standard formulation of the microscopic model employed here. This formulation or some of its parts have been presented in a similar way in other papers. This line of thought follows the still interesting work of Agin et al. during the 1960s [31], continued by Cammarata [32-34], crystallized in the work of Peradejordi [35] and extended by one of us [36-42]. The last paper not belonging to our group, and using the model we are employing here was published in 1979 [43]. We are doing so to differentiate it unambiguously from the statistics-backed methodologies.

Let us consider the state of thermodynamic equilibrium, and a 1:l stoichiometry in the formation of the drug-receptor complex [37]:

$$D_i + R \square \quad D_i R \tag{1}$$

where $D_i$ is the drug, R is the receptor, and $D_iR$ is the drug-receptor complex. According to statistical thermodynamics the equilibrium constant, $K_i$, is expressed as:

$$K_i = \frac{Q_{D_iR}}{Q_{D_i} Q_R} \exp(-\Delta\varepsilon_0^i / kT) \tag{2}$$

where $\Delta\varepsilon_0^i$ is the difference between the ground-state energy of $D_iR$ and the energies of the ground states of $D_i$ and R:

$$\Delta\varepsilon_0^i = \varepsilon_{D_iR} - (\varepsilon_{D_i} + \varepsilon_R) \tag{3}$$

and the Q's are the total partition functions (PF) measured from the ground state (in solution). T and k are the temperature and the Boltzmann constant, respectively. Using well-grounded approximations we may write Eq. 2 in logarithmic form as:

$$\log K_i = a + bM_{D_i} + c\log\left[\sigma_{D_i} / (ABC)^{1/2}\right] + d\Delta\varepsilon_i \tag{4}$$

Where a, b, c and d are constants, M is the drug's mass, σ its symmetry number and ABC the product of the drug's moment of inertia about the three principal axes of rotation.

The interaction energy, $\Delta\varepsilon_i$ , cannot be determined directly, either due to the size of the receptor or to the lack of knowledge of its molecular structure. As we are dealing with a weak drug-receptor interaction, we can employ Perturbation Theory in the Klopman-Hudson form to estimate $\Delta\varepsilon_i$ [44,45]. According to this method, the change in electron energy, ΔE, associated with the interaction of atoms i and j is:

$$\Delta E = \sum_p \left[ Q_i Q_j / R_{ij} + (1/2)(\beta_{ij}^2) \sum_m \sum_n D_{mi} D_{n'j} / (E_m - E_{n'}) - (1/2)(\beta_{ij}^2) \sum_m \sum_{n'} D_{m'i} D_{nj} / (E_{m'} - E_n) \right] \tag{5}$$

Where $Q_i$ is the net charge of atom *i,* $D_{mi}$ is the orbital charge of atom *i* in the MO *m,* $\beta_{ij}$ is the resonance integral; and $E_m$ ($E_{m'}$) is the energy of the m-th (m'-th) occupied (virtual) MO of the drug, n and n' standing for the receptor. The value of $\beta_{ij}$ is kept independent of the kind of AO because the drug-receptor complex does not involve covalent bonds. The summation on p is over all pairs of interacting atoms of the drug and the receptor.

The first term of the right side of Eq. 5 represents the electrostatic interaction between two atoms having net charges $Q_i$ and $Q_j$. The second and third terms introduce the interactions between the occupied and empty MOs of the drug and those of the receptor. Noting that $1/(E_m-E_{n'})$ and similar terms can be written in the form 1/(1-x), we may expand them as a convergent infinite series. With this treatment we obtain [42]:

$$\Delta E = a + \sum_i \left[ e_i Q_i + f_i S_i^E + s_i S_i^N \right] + \sum_i \sum_m \left[ h_i(m) F_i(m) + j_i(m) S_i^E(m) \right] +$$
$$+ \sum_i \sum_{m'} \left[ r_i(m') F_i(m') + t_i(m') S_i^N(m') \right] + \Phi \tag{6}$$

Where a, e, f, g, h, j, r and t are constants and the summation on i is now only over the drug's atoms. $S_i^E$ and $S_i^N$ are, respectively, the total atomic electrophilic and nucleophilic superdelocalizabilities of Fukui et al. $F_{i,m}$ is the Fukui index of atom i in occupied (empty) MO m (m') [46]. The total atomic electrophilic superdelocalizability (ESD) of atom i is defined as:

$$S_i^E = \sum_m F_{i,m} / E_m = \sum_m S_i^E(m) \tag{7}$$

Where the summation on m runs only over the occupied MOs. $S_i^E(m)$ is called the orbital electrophilic superdelocalizability of atom i at MO m.

The total atomic nucleophilic superdelocalizability (NSD) of atom i is defined as:

$$S_i^N = \sum_{m'} F_{i,m'} / E_{m'} = \sum_{m'} S_i^N(m') \tag{8}$$

where the summation on m' runs only over the empty MOs. $S_i^N(m')$ is called the orbital nucleophilic superdelocalizability of atom i at MO m'. Φ stands for the remaining series expansion terms. The summation on p is hidden for the sake of clarity. $S_i^E$ is associated with the total electron-donating capacity of atom i and $S_i^N$ with its total electron-accepting capacity. These indices are very useful to compare the reactivity of a similar atomic position through a series of molecules because they incorporate the eigenvalue spectrum which is usually different in each molecular system. The orbital components, $S_i^E(m)$ and $S_i^N(m')$, become significant when fine aspects of the drug-receptor interaction are needed for a more complete explanation.

The most important characteristic of Eq. 6. is that it includes terms belonging just to the drug molecule. Recently we analyzed several terms composing Φ, finding that we may associate several of them with a set of local atomic reactivity indices recently proposed by one of us. These indices are:

The local atomic electronic chemical potential of atom i, $\mu_i$, defined as:

$$\mu_i = \frac{E_{oc}^* - E_{em}^*}{2} \tag{9}$$

Where $E_{oc}^*$ is the upper occupied MO with a non-zero Fukui index and $E_{em}^*$ is the lowest empty MO with a non-zero Fukui index. $\mu_i$ is a measure of the propensity of a system to acquire or lose electrons; a large negative value indicates a good electron acceptor while a small negative value implies a good electron donor. Note that $\mu_i$ is the midpoint between the local HOMO and LUMO of atom i.

The local atomic hardness of atom i, $\eta_i$, is defined as:

$$\eta_i = E^*_{em} - E^*_{oc} \tag{10}$$

$\eta_i$ is the gap between the local HOMO and LUMO energies of atom i and can be interpreted as the resistance to exchange electrons with the surroundings. The local atomic softness of atom i, $\varsigma_i$, is defined as the inverse of the local atomic hardness.

The local electrophilic index of atom i, $\omega_i$, is defined as:

$$\omega_i = \frac{\mu_i^2}{2\eta_i} \tag{11}$$

The maximal amount of electronic charge that an electrophile may accept, $Q_i^{\max}$ , is defined as:

$$Q_i^{\max} = \frac{-\mu_i}{\eta} \tag{12}$$

The local electrophilic index is associated with the electrophilic power and includes the tendency of the electrophile to accept extra electronic charge together with its resistance to exchange charge with the medium.

From the theoretical viewpoint it is very important to stress that these local atomic reactivity indices were obtained directly from Molecular Orbital (MO) Theory and not from Density Functional Theory (DFT). These indices have the same units as the global DFT indices (i.e., eV), having therefore an analogous meaning. On the other hand, the local reactivity indices coming directly from DFT are, in general, the global DFT ones multiplied by an electron population. These local indices have eV·e as units and are therefore not equivalent in meaning to the ones coming from MO theory.

The introduction of Eq. 6 and 9 to 12 into Eq. 4 leads to the final equation:

$$\begin{aligned}\log K_i = a + bM_{D_i} + c\log\left[\sigma_{D_i}/(ABC)^{1/2}\right] + \sum_j \left[e_j Q_j + f_j S_j^E + s_j S_j^N\right] + \\ + \sum_j \sum_m \left[h_j(m) F_j(m) + x_j(m) S_j^E(m)\right] + + \sum_j \sum_{m'} \left[r_j(m') F_j(m') + t_j(m') S_j^N(m')\right] + \\ + \sum_j \left[g_j \mu_j + k_j \eta_j + o_j \omega_j + z_j \varsigma_j + w_j Q_j^{\max}\right]\end{aligned} \tag{13}$$

Then, for n (i = 1,..,n) molecules we have a set of n simultaneous equations 13. In theory, this system of simultaneous equations holds for the atoms j of the molecule directly perturbed by their interaction with the receptor. Combined with the standard multiple-regression techniques, these equations can be advantageously applied to estimate the relative variation of log $K_i$ in a family of molecules. Also, they can be used to find out which atoms are directly concerned in the formation of the drug-receptor complex. Here statistical analysis is used, not to see whether there is a structure-activity relationship, but to find the best one.

It was possible to show that the moment of inertia term can be expressed as [39,40]:

$$\log\left[(ABC)^{-1/2}\right] = \sum_t \sum_t m_{i,t} R_{i,t}^2 = \sum_t O_t \quad (14)$$

where the summation over t is over the diverse substituents of the molecule, $m_{i,t}$ is the mass of the i-th atom belonging to the t-th substituent, $R_{i,t}$ being its distance to the atom to which the substituent is bonded. This approximation allows us to convert a molecular property into a sum of substituent properties. As the physical interpretation of the *Ot* terms, it was proposed that they correspond to the fraction of molecules attaining the correct orientation to interact with the receptor. We called them Orientation Parameters. The success of this method was appreciated when it was applied to a great variety of drug-receptor systems [36, 39,47-61].

Now, to deal with biological activities that are not equilibrium constants, we used Cammarata's results [62-64] and stated the following hypothesis: all biological processes occurring, from the instant of the entry of a drug molecule into the biological system (*In vitro* or *In vivo*) until the manifestation of any biological activity, are controlled by the local atomic reactivity indices appearing in Eq. 13. Consequently, if this hypothesis is right, a preliminary representation of the ultimate biological action can be obtained merely by replacing log $K_i$ by log (BA), where BA can be any biological activity. This extension of the method has produced very interesting results [65-67]. We shall work within the common skeleton hypothesis stating that there is a definite group of atoms, common to all molecules analyzed, that accounts for almost all the variation of the biological activity. The effect of the substituents consists in modifying the electronic structure of this skeleton and/or influencing the correct placement of the drug throughout the orientational parameters.

## 2.2 Delection of the Experimental Data

Two sets of experimental data were considered here. The first one is the *In vitro* toxicity (reported as $IC_{50}$, [21]) in a cell-based assay using a human tumor cell line derived from human prostate cancer (DU145, [68]) . The second set is the same activity but on a human myelogenous leukemia cell line (K562, [69,70]). Cytotoxicity was measured as follows: the cells were grown in either DMEM or RPMI supplemented with 10% fetal bovine serum and 1unit/mL penicillin–streptomycin solution. The tumor cells were plated into six well dishes at a cell density of 1.0×105 cells/mL/well, and compounds were added 24h later at various concentrations. Cell counts were determined from duplicate wells after 96h of treatment. The total number of viable cells was determined by trypan blue exclusion (from [21]). The selected molecules are shown in Fig. 1 and Table 1. The numbers in Fig. 1 correspond to the common skeleton selected for this study.

## 2.3 Calculations

The electronic structure of all molecules was calculated within Density Functional Theory at the B3LYP/6-31g (d,p) level of theory. The Gaussian package of programs was used [71]. After full geometry optimization all the information necessary to get numerical values for all the local atomic reactivity indices of Eq. 13 was extracted from the Gaussian results with software written in our Unit. Negative electron populations coming from Mulliken Population Analysis were corrected [72]. Molecular orbitals and Molecular Electrostatic Potentials (MEP) were depicted using GaussView. Orientational parameters were calculated as usual [39,40]. We made use of Linear Multiple Regression Analysis (LMRA) techniques to find the best solution. For each case, a matrix containing the dependent variable (the logarithm of $IC_{50}$)

and the local atomic reactivity indices of all atoms of the common skeleton as independent variables was built. Statistica software was used for LMRA [73].

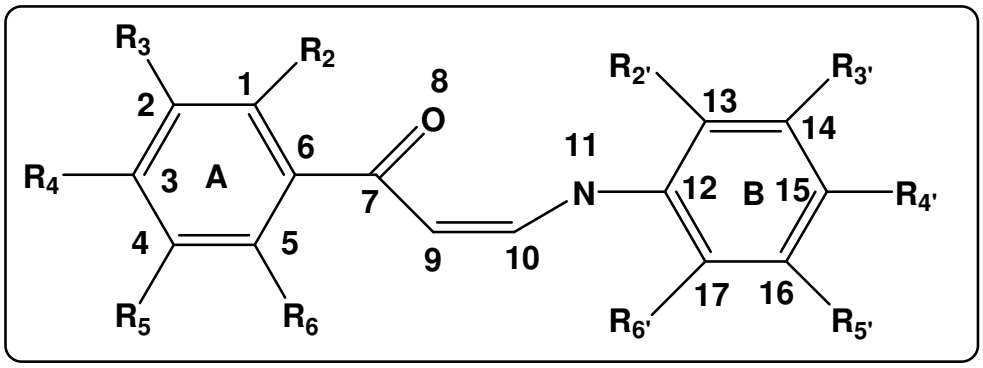


**Fig. 1. (*Z*)-1-Aryl-3-arylamino-2-propen-1-one derivatives**

**Table 1. (*Z*)-1-Aryl-3-arylamino-2-propen-1-one derivatives and their cytotoxicity**

| | $R_2$ | $R_3$ | $R_4$ | $R_5$ | $R_6$ | $R_{2'}$ | $R_{3'}$ | $R_{4'}$ | $R_{5'}$ | $R_{6'}$ | log($IC_{50}$) (μM) DU145 | log($IC_{50}$) (μM) K562 |
|---|---|---|---|---|---|---|---|---|---|---|---|---|
| 1 | H | H | OMe | H | H | H | H | OMe | H | H | 1.88 | 2 |
| 2 | H | H | OMe | H | H | H | OMe | OMe | OMe | H | 1.70 | 1.88 |
| 3 | OMe | H | OMe | H | OMe | H | H | OMe | H | H | 1.88 | 1.88 |
| 4 | OMe | H | OMe | H | OMe | OH | H | H | H | H | 1.40 | 1.88 |
| 5 | OMe | H | OMe | H | OMe | H | H | Cl | H | H | 1.40 | 1.40 |
| | OMe | H | OMe | H | OMe | OMe | H | OMe | H | H | 1.88 | 1.88 |
| 7 | OMe | H | OMe | H | OMe | OMe | H | OMe | H | OMe | 1.88 | 1.78 |
| 8 | OMe | H | OMe | H | OMe | H | OMe | OMe | OMe | H | 1.5 | 1.88 |
| 9 | H | OMe | OMe | OMe | H | OH | H | H | H | H | -0.60 | -0.30 |
| 10 | H | OMe | OMe | OMe | H | H | OH | H | H | H | -0.12 | -0.30 |
| 11 | H | OMe | OMe | OMe | H | OMe | H | H | H | H | 0.40 | 0.40 |
| 12 | H | OMe | OMe | OMe | H | H | H | OMe | H | H | -0.30 | -0.30 |
| 13 | H | OMe | OMe | OMe | H | H | H | Cl | H | H | -0.30 | -0.60 |
| 14 | H | OMe | OMe | OMe | H | H | H | $OCF_3$ | H | H | 0.48 | 1.30 |
| 15 | H | OMe | OMe | OMe | H | H | H | $CF_3$ | H | H | -0.3 | -0.30 |
| 16 | H | OMe | OMe | OMe | H | H | OH | OMe | H | H | -1 | -1 |
| 17 | H | OMe | OMe | OMe | H | H | $NH_2$ | OMe | H | H | -1 | -0.60 |
| 18 | H | OMe | OMe | OMe | H | H | F | OMe | H | H | -0.60 | -0.60 |
| 19 | H | OMe | OMe | OMe | H | H | Cl | OMe | H | H | -0.70 | -0.60 |
| 20 | H | OMe | OMe | OMe | H | Cl | H | H | OH | H | -0.12 | 0.40 |
| 21 | H | OMe | OMe | OMe | H | OMe | H | OMe | H | OMe | 1.88 | 1.90 |
| 22 | H | OMe | OMe | OMe | H | H | OMe | OMe | OMe | H | 1.60 | 1.40 |
| 23 | Br | OMe | OMe | OMe | H | OH | H | H | H | H | -0.60 | -0.70 |
| 24 | Br | OMe | OMe | OMe | H | H | H | OMe | H | H | -0.70 | -0.60 |
| 25 | Br | OMe | OMe | OMe | H | H | OH | OMe | H | H | -1.22 | -1 |
| 26 | Cl | OMe | OMe | OMe | H | H | OH | OMe | H | H | -0.70 | -0.60 |
| 27 | $NO_2$ | OMe | OMe | OMe | H | H | H | OMe | H | H | -0.22 | -0.22 |

## 3. RESULTS

### 3.1 Correlation between the Reported Experimental Values

We have found that there is a high correlation between the two sets of experimental values. The relationship has the following form:

$$\log(IC_{50-K562}) = 0.11 + 0.99\log(IC_{50-DU145}) \tag{15}$$

With n=27, R=0.98, $R^2$=0.95, adj $R^2$=0.95 and SD=0.25 (see Fig. 2). This does not necessarily imply that the SAR equations are the same for both sets (see below). Note that some points lie outside the 95% confidence interval.

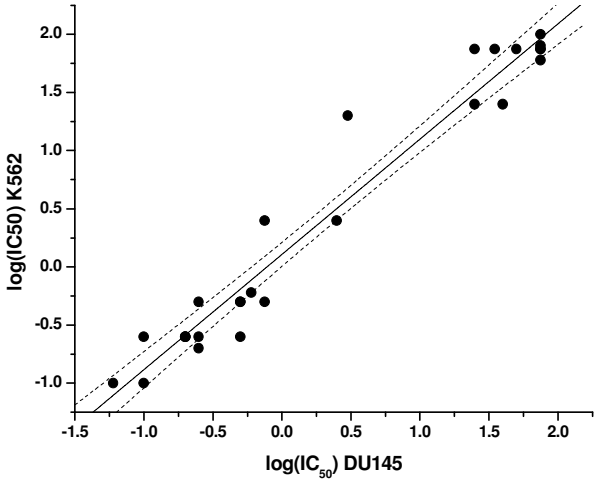


**Fig. 2. Correlation between experimental values of log ($IC_{50}$) of DU145 and K562 cell lines. Dashed lines denote the 95% confidence interval**

### 3.2 Results for the DU-145 Cell Line

It was not possible to find any statistically significant relationship for the whole set of molecules (n=27). Examining Table 1 we noticed that the reported toxicity values can be separated into two subsets. One set comprises those molecules having very high values of $\log(IC_{50})$ and the other included molecules with very high toxicity. Next, we worked with the hypothesis that the high toxicity might have a distinct action mechanism. Then we discarded the set comprising molecules 1-8, 21 and 22 of Table 1 and centered our attention on the remaining ones (n=17). For this set the following equation was obtained:

$$\log(IC_{50}) = -7.11 + 8.14Q_5^{\max} + 1.25F_{14}(HOMO-1)^* + 0.01\Theta_{R2} - 1.18F_{16}(LUMO+1)^* + \\ +0.30S_2^E(HOMO)^* + 0.01S_4^N(LUMO)^* \tag{16}$$

With n=17, R=0.97, $R^2$=0.95, adj $R^2$=0.92, F(6,10)=30.35 (p<0.00001), outliers>2σ=0 and SD=0.13. Here, $\Theta_{R2}$ is the orientational parameter of the $R_2$ substituent, $Q_5^{\max}$ is the maximal amount of electronic charge atom 15 may accept, $F_{14}(HOMO-1)*$ is the Fukui index (the electron population) of the second highest occupied MO localized on atom 14, $F_{16}(LUMO+1)*$ is the Fukui index of the second empty MO localized on atom 16, $S_2^E(HOMO)*$ is the orbital electrophilic superdelocalizability of the highest occupied MO localized on atom 2 and $S_4^N(LUMO)*$ is the orbital nucleophilic superdelocalizability of the highest empty MO localized on atom 4. The beta coefficients and t-test for significance of coefficients of Eq. 16 are shown in Table 2. Concerning independent variables, Table 3 shows that there are no significant internal correlations with the exception of $r^2\{\Theta_{R2}, S_2^E(HOMO)*\}$=0.37 and $r^2\{\Theta_{R2}, S_2^E(HOMO)*\}$=0.35. Fig. 3 shows the plot of observed values *vs.* calculated ones. The associated statistical parameters of Eq. 16 show that this equation is statistically significant and that the variation of a group of local atomic reactivity indices belonging to the common skeleton explains about 92% of the variation of the biological activity.

**Table 2. Beta coefficients and *t*-test for significance of coefficients in Eq. 16**

| | Beta | t(10) | p-level |
|---|---|---|---|
| $Q_5^{\max}$ | 0.72 | 7.31 | <0.00003 |
| $F_{14}(HOMO-1)*$ | 0.47 | 5.59 | <0.0002 |
| $\Theta_{R2}$ | 0.97 | 8.66 | <0.000006 |
| $F_{16}(LUMO+1)*$ | -0.53 | -4.36 | <0.001 |
| $S_2^E(HOMO)*$ | 0.48 | 5.19 | <0.0004 |
| $S_4^N(LUMO)*$ | 0.29 | 3.27 | <0.008 |

**Table 3. Squared correlation coefficients for the variables appearing in Eq. 16**

| | $Q_5^{\max}$ | $F_{14}(HOMO-1)*$ | $\Theta_{R2}$ | $F_{16}(LUMO+1)*$ | $S_2^E(HOMO)*$ |
|---|---|---|---|---|---|
| $F_{14}(HOMO-1)*$ | 0.07 | 1.00 | | | |
| $\Theta_{R2}$ | 0.002 | 0.02 | 1.00 | | |
| $F_{16}(LUMO+1)*$ | 0.29 | 0.10 | 0.35 | 1.00 | |
| $S_2^E(HOMO)*$ | 0.01 | 0.05 | 0.37 | 0.18 | 1.00 |
| $S_4^N(LUMO)*$ | 0.16 | 0.04 | 0.005 | 0.12 | 0.005 |

## 3.3 Results for the K562 Cell Line

In this case it was not possible to find any statistically significant relationship for the whole set of molecules (n=27). As in the previous section we analyzed only the set of highly toxic molecules (n=17). For this case the following equation was obtained:

$$\log(IC_{50}) = -4.39 + 2.32F_{16}(HOMO-1)^{*} + 0.31S_{14}^{E}(HOMO-2)^{*} - 32.85\mu_{17} - -0.99F_{17}(HOMO-1)^{*} \quad (17)$$

With n=17, R=0.87, $R^2$=0.77, adj $R^2$=0.69, F(4,12)=9.77 (p<0.0009), outliers>2σ=0 and SD=0.32. Here, $\mu_{17}$ is the local electronic chemical potential of atom 17, $F_{16}(HOMO-1)^{*}$ is the Fukui index of the second highest occupied MO localized on atom 16, $F_{17}(HOMO-1)^{*}$ is the Fukui index of the second highest occupied MO localized on atom 17 and $S_{14}^{E}(HOMO-2)^{*}$ is the orbital atomic electrophilic superdelocalizability of the third highest occupied MO localized on atom 14. The beta coefficients and t-test for significance of coefficients of Eq. 17 are shown in Table 4. Concerning independent variables, Table 5 shows that there are no significant internal correlations. Fig. 4 shows the plot of observed values vs. calculated ones. The associated statistical parameters of Eq. 17 show that this equation is statistically significant and that the variation of a group of local atomic reactivity indices belonging to the common skeleton explains about 69% of the variation of the biological activity.

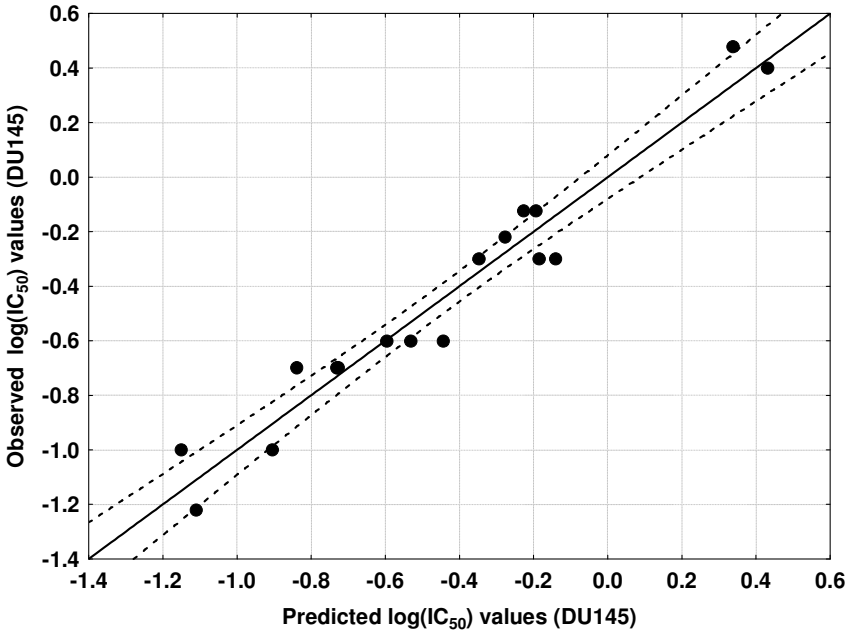


**Fig. 3. Observed *vs.* calculated values (Eq. 16) of log ($IC_{50}$). Dashed lines denote the 95% confidence interval**

**Table 4. Beta coefficients and *t*-test for significance of coefficients in Eq. 17**

| | Beta | t(12) | p-level |
|---|---|---|---|
| $F_{16}(HOMO-1)*$ | 0.60 | 4.29 | <0.001 |
| $S_{14}^{E}(HOMO-2)*$ | 0.39 | 2.62 | <0.02 |
| $\mu_{17}$ | -0.34 | -2.40 | <0.03 |
| $F_{17}(HOMO-1)*$ | -0.28 | -1.90 | <0.08 |

**Table 5. Squared correlation coefficients for the variables appearing in Eq. 17**

| | $F_{16}(HOMO-1)*$ | $S_{14}^{E}(HOMO-2)*$ | $\mu_{17}$ |
|---|---|---|---|
| $S_{14}^{E}(HOMO-2)*$ | 0.0004 | 1.00 | |
| $\mu_{17}$ | 0.005 | 0.005 | 1.00 |
| $F_{17}(HOMO-1)*$ | 0.0009 | 0.12 | 0.006 |

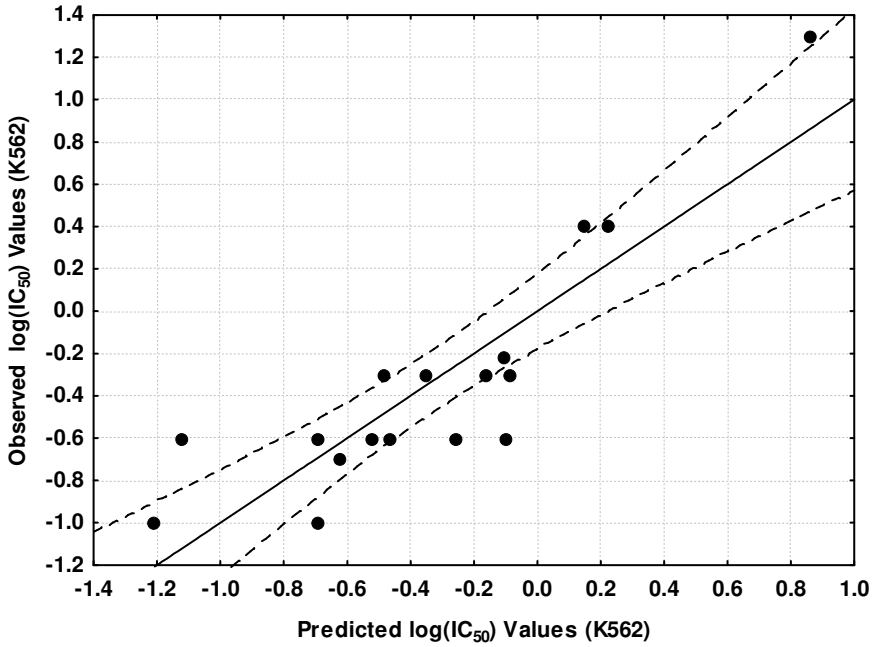


**Fig. 4. Observed *vs.* calculated values (Eq. 17) of log ($IC_{50}$). Dashed lines denote the 95% confidence interval**

## 4. DISCUSSION

### 4.1 Molecular Electrostatic Potential

The fully optimized structures of these molecules show that we are in the presence of two aromatic regions connected in different ways. The region comprising ring A is separated from the ring B region by a chain allowing π-electron transfer only in the case of coplanarity

of the whole system. The nature of the $R_2$, $R_6$, $R'_2$ and $R'_6$ substituents could produce steric hindrance (think of the biphenyl case) preventing the coplanarity of rings A and B. Considering that at body temperature (provided that there are no high energy barriers) these molecules can reach any conformation up to 7 kcal/mol from the fully optimized structure, we have no clear basis to propose what the three-dimensional conformation might be at each step of the process leading to the biological activity. Fig. 5 shows the MEP of molecule 9 (Table 1), a coplanar system.

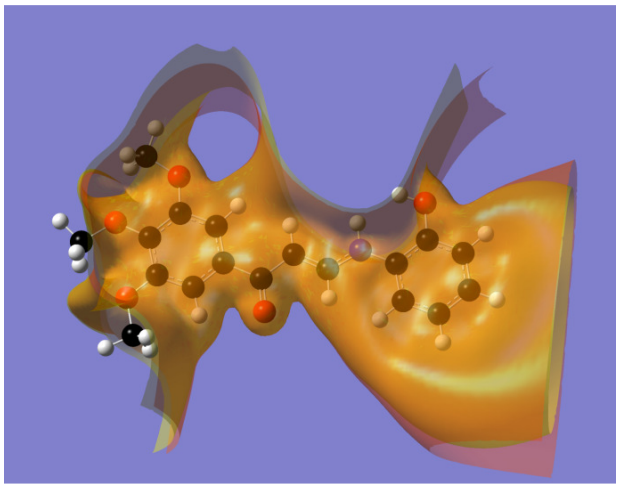

**Fig. 5. Molecular electrostatic potential of molecule 9. The orange isovalue surface corresponds to negative MEP values (-0.0004) and the yellow isovalue surface to positive MEP values (0.0004)**

In the left and upper parts of molecule 9 we may appreciate a region of positive MEP. Another region of positive MEP exists at the right side of Fig. 5 surrounding ring B. The region of negative MEP encompasses the whole π system. Fig. 6 shows the MEP of molecule 27, a non-coplanar system.

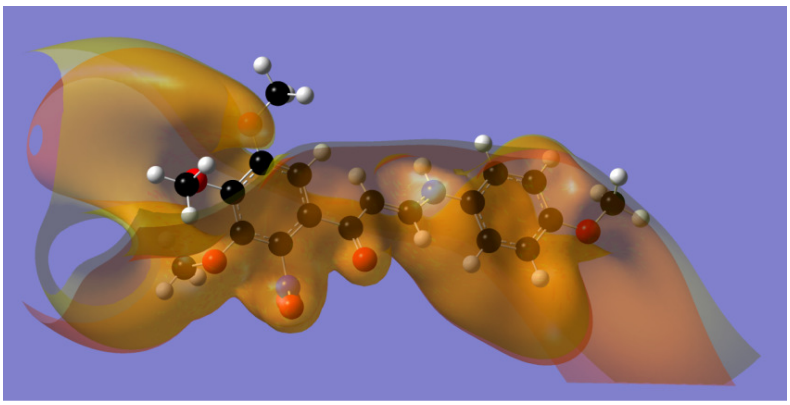

**Fig. 6. Molecular electrostatic potential of molecule 27. The orange isovalue surface corresponds to negative MEP values (-0.0004) and the yellow isovalue surface to positive MEP values (0.0004)**

We may appreciate that the MEP structure of molecule 27 is significantly different from the MEP of molecule 9. The changes in the MEP structure are due to the nitro (ring A) and methoxy (ring B) substituents. In drug-receptor theory it is suggested that there is a zone in which an accumulation, recognition and guidance of the drug molecule towards the receptor occurs through long-range interactions. The recognition process can be associated with the matching of the MEP of the drug and the receptor to produce a correct geometrical alignment. Then, one way of reaching a decision about the behavior of the MEP during the processes leading to biological activity is to take a molecule to analyze the behavior of the MEP in the conformational space around the fully optimized structure and to compare it with other similar molecules and with compounds acting in the same way but having a different chemical constitution. It is worth mentioning that the complex structure of the MEP in several systems (exceptions could be, for example, dopamine and glycine ligands [53,74] seems to be the result of evolution and selection.

## 4.2 Localization of Molecular Orbitals

Fig.7 and 8 show, respectively, the HOMO and LUMO of molecule 12.

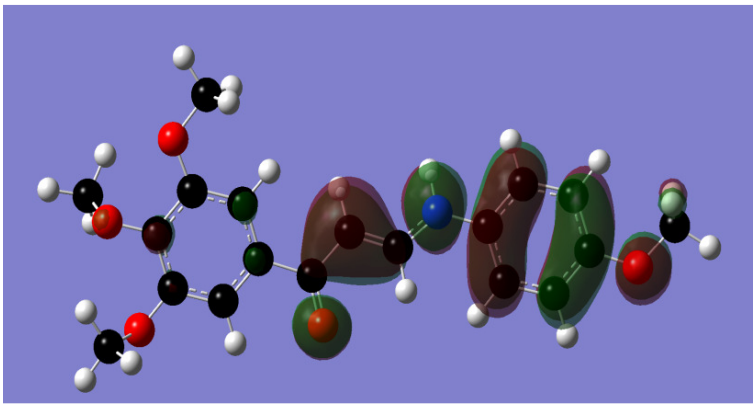

**Fig. 7. Localization of the highest occupied molecular orbital (HOMO) of molecule 12 (isovalue = 0.02)**

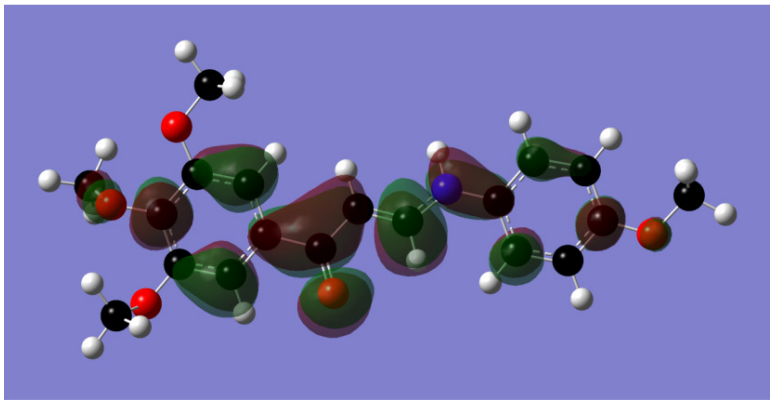

**Fig. 8. Localization of the lowest empty molecular orbital (LUMO) of molecule 12 (isovalue = 0.02)**

The HOMO of molecule 12 is localized on ring B and on the chain connecting both phenyl rings. This MO is of π nature. The LUMO is localized mainly on ring A and on the connecting chain but also on ring B. It is also of π nature. Note that, in ring B, the LUMO is not localized on all the atoms of the phenyl ring. To appreciate the importance of localization let us assume that molecule 12 participates in an interaction requiring that ring A donates π electrons through a π MO. As the HOMO is not localized on ring A, this electron donation will occur through the highest π MO located on ring A which does not coincide with the molecular HOMO. These facts are the basis for building the matrix of independent variables and provide the logics underlying our use of local atomic reactivity indices. Fig. 9 and 10 show, respectively, the HOMO and LUMO of molecule 9.

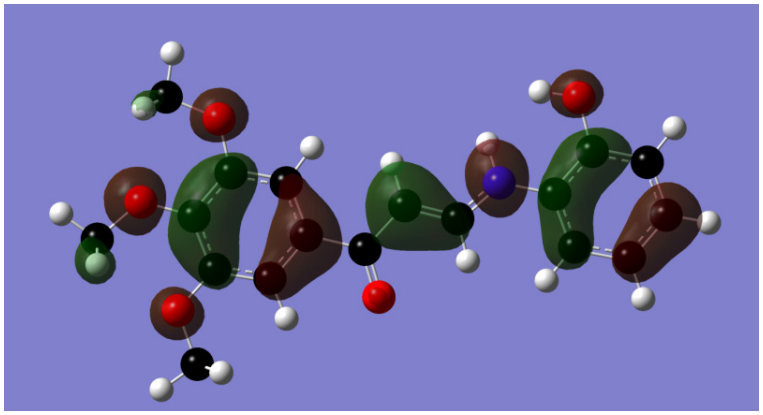

**Fig. 9. Localization of the highest occupied molecular orbital (HOMO) of molecule 9 (isovalue = 0.02)**

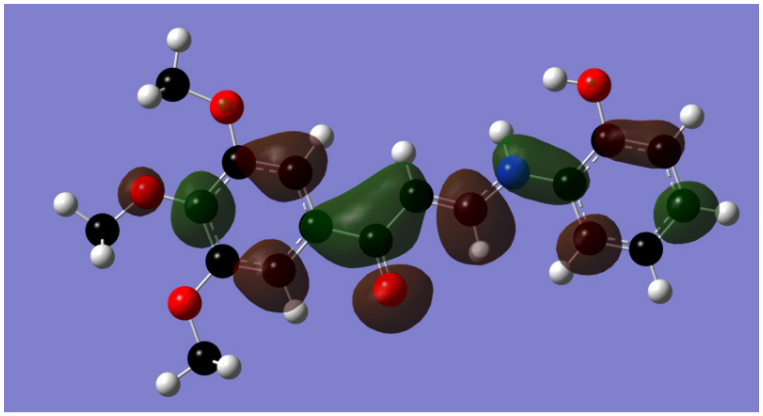

**Fig. 10. Localization of the lowest empty molecular orbital (LUMO) of molecule 9 (isovalue = 0.02)**

In this case the HOMO is localized over all the π system with the exception of a carbon atom of ring B (Fig. 9). Note that in the case of molecule 12 (Fig. 7) the HOMO is localized over all the carbon atoms of ring B. These apparently small differences can become very important in regulating binding and activity. The LUMO of molecule 9 is also localized over all the π system and is very similar to the LUMO of molecule 12.

### 4.3 Relationships between Structure and Activity for the DU-145 Cell Line

Equation 16 shows that there is a significant relationship between the variation of cytotoxicity and the variation of the numerical values of a set of local atomic reactivity indices belonging to certain atoms of the common skeleton. The Beta values (Table 2) indicate that the importance of variables is $\Theta_{R2} > Q_5^{\max} > F_{16}(LUMO+1)^* > F_{14}(HOMO-1)^* = S_2^E(HOMO)^* > S_4^N(LUMO)^*$. Table 3 shows that there is a certain degree of correlation between $\Theta_{R2}$ and $F_{16}(LUMO+1)^*$, and between $\Theta_{R2}$ and $S_2^E(HOMO)^*$. We cannot provide for the moment an explanation of the fact that $\Theta_{R2}$ is a purely geometrical index (it is only mass- and distance-dependent) while $F_{16}(LUMO+1)^*$ and $S_2^E(HOMO)^*$ are purely electronic ones. Fig. 3 shows that only a few points lie just outside the 95% confidence limit. This is a good indication that the common skeleton hypothesis works well for this case. The standard error of estimate is 0.13, a value that is lower than those normally obtained in theoretical studies of 1:1 *In vitro* drug-receptor interaction. Note that the abovementioned internal correlations might make some contributions to lower the SD value.

A variable-by-variable analysis suggests that high cytotoxicity is associated with low values of $Q_5^{\max}$, $F_{14}(HOMO-1)^*$, $\Theta_{R2}$ and $S_4^N(LUMO)^*$; and high values for $F_{16}(LUMO+1)^*$ and $S_2^E(HOMO)^*$. A low value for $Q_5^{\max}$ is associated with a negative net charge on atom 5 (which is the case in these molecules), with high values for $\eta_5$ (a case only found in H atoms) or with a highest occupied local MO of σ nature (not the actual case). A low value for $S_4^N(LUMO)^*$ is associated with a low localization of the molecular LUMO on this atom (see Fig. 10 for molecule 9). We suggest that atom 4 is participating as an electron donor center. A high numerical value for $S_2^E(HOMO)^*$ indicates that atom 2 is also participating as an electron donor center (see Fig. 9 for molecule 9). Note that the molecular LUMO also has a low localization on this atom (Fig. 10 for molecule 9). For the case of molecule 12, we may see in Fig. 11 that atoms 2 and 4 are donating electrons from the second highest occupied molecular MO (corresponding to the first highest occupied local MO* for atoms 2 and 4 in this molecule). It is likely that both atoms, 2 and 4, participate interacting at the same time with a π electron center.

A low value for $\Theta_{R2}$ is an indication that the $R_2$ substituent should be of the size of an H or Cl atoms. The only way to analyze carefully the optimal value for $\Theta_{R2}$ is by synthesizing and testing a series of molecules in which only one substituent is varied at a time. This will generate the input for new theoretical studies leading to a better understanding of this phenomenon. A high value for $F_{16}(LUMO+1)^*$ suggests that atom 15 participates as an electron acceptor center. $F_{16}(LUMO)^*$ also participates but, given that the localization of the local LUMO* on these atoms is low, its contribution does not appear in Eq. 16.

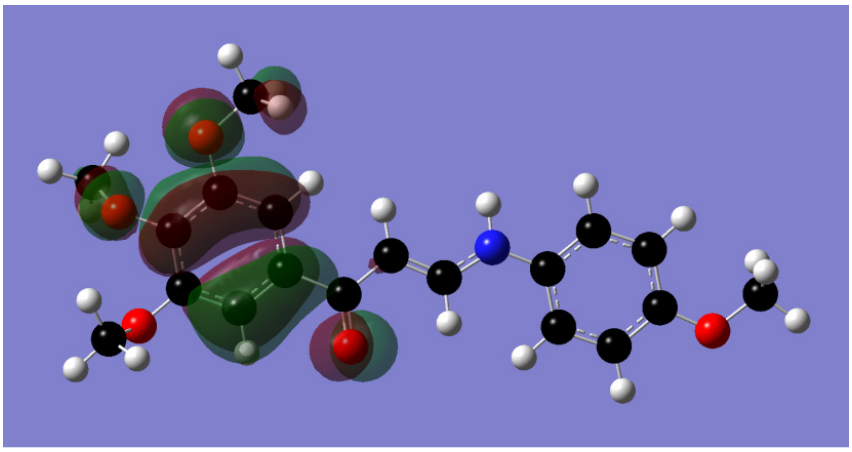

**Fig. 11. Localization of the second highest occupied molecular orbital (HOMO-1) of molecule 12 (isovalue = 0.02)**

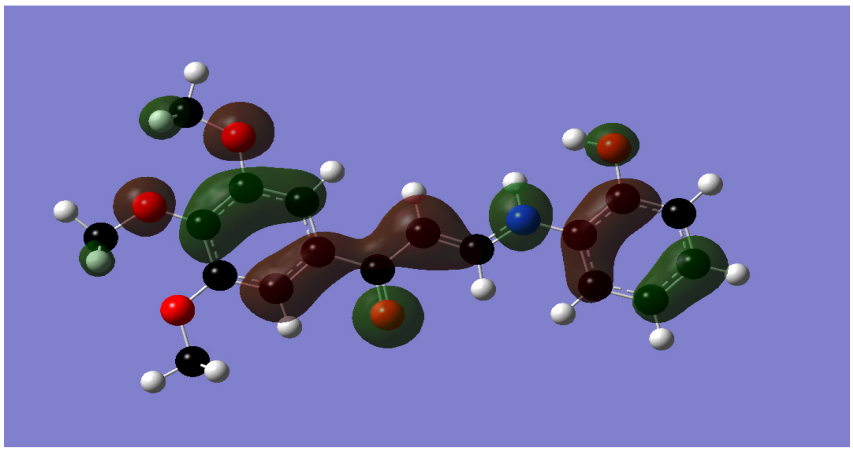

**Fig. 12. Localization of the second highest occupied molecular orbital (HOMO-1) of molecule 9 (isovalue = 0.02)**

A low value required for $F_{14}(HOMO-1)^*$ demands a short discussion. Fig. 7 shows that in the case of molecule 12 the molecular HOMO is localized on atom 14. In molecule 9 this is not the case (Fig. 9). In molecules 9 and 12 the second highest occupied molecular orbital, HOMO-1, also skips atom 14. In molecule 9, the local HOMO* coincides with the molecule's HOMO-4. We suggest that high toxicity seems to be related to the electron-accepting capacity of atom 14. Ring A appears to act as an electron donor center while ring B seems to act as an electron acceptor. The whole process is charge-, orbital- and sterically-controlled. All the above suggestions are summarized in the two-dimensional (2D) toxicity pharmacophore shown in Fig. 13. It is important to notice that no local atomic reactivity indices appear in eq. 16. Therefore, we have no information to discern if this chain acts merely as a linker between the phenyl rings, serves for electron movement between the phenyl rings (via substitutions), or both.

### 4.4 Relationships between Structure and Activity for the K-562 Cell Line

The best equation obtained is statistically significant but it lacks good predictive quality. It explains only 69% of the variation of toxicity against the K562 cell line. Moreover, the SD value is too high (0.32), a fact reflected in Fig. 4. Notice that variables belonging only to ring B appear in Eq. 17. Atoms 14 and 16 seem to be involved in controlling toxicity as in the previous case. Atom 17 is represented by $\mu_{17}$ and $F_{17}(HOMO-1)^*$, both indicating that it acts as an electron donor. Because of these results we shall refrain from discussing Eq. 17 with further details and presenting a pharmacophore. How can we explain these bad results? If we accept that the experimental results are correct we might be in the presence of two different toxicity mechanisms. Unhappily there are not enough molecules in the set to test this hypothesis.

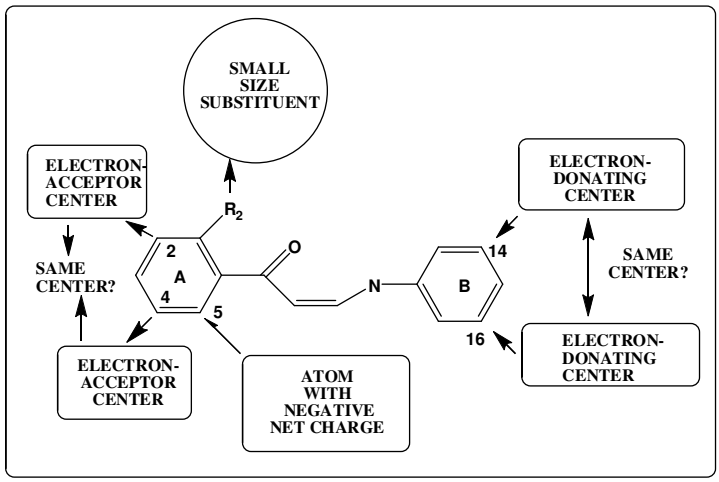


**Fig. 13. 2D pharmacophore for toxicity of (*Z*)-1-aryl-3-arylamino-2-propen-1-one derivatives against the DU-145 cell line**

## 5. CONCLUSIONS

We have obtained statistically significant results relating the variation of a definite set of local atomic reactivity indices to the variation of toxicity against the DU-145 cell line for a series of (*Z*)-1-aryl-3-arylamino-2-propen-1-one derivatives. No local atomic reactivity indices belonging to the chain joining phenyl rings A and B appear in the final equation. Therefore it is not possible to elaborate about its role. Rings A and B seem to play opposite roles regarding electron transfer. The whole process is charge-, orbital- and steric-controlled. No good results were obtained for the K562 cell line. More experimental information is needed to clarify this last result.

## COMPETING INTERESTS

The authors have no financial and personal relationships with other people or organizations that could inappropriately influence their work.

## REFERENCES


1. Oakley CE, Oakley BR, Identification of [gamma]-tubulin, a new member of the tubulin superfamily encoded by mipA gene of Aspergillus nidulans, Nature. 1989;338:662-664.
2. Keeling PJ, Doolittle WF, Alpha-tubulin from early-diverging eukaryotic lineages and the evolution of the tubulin family, Mol. Biol. Evol. 1996;13:1297-1305.
3. Nogales E, Wolf SG, Downing KH, Structure of the [alpha][beta] tubulin dimer by electron crystallography, Nature. 1998;391:199-203.
4. Ludueña RF, A hypothesis on the origin and evolution of tubulin, Int. Rev. Cell. Mol. Biol. 2013;302:41-185.
5. Jordan A, Hadfield JA, Lawrence NJ, McGown AT, Tubulin as a target for anticancer drugs: Agents which interact with the mitotic spindle, Med. Chem. rev. 1998;18:259-296.
6. Pellegrini F, Budman DR, Review: Tubulin Function, Action of Antitubulin Drugs, and New Drug Development, Cancer Inv. 2005;23:264-273.
7. Li W, Drugs Targeting Tubulin Polymerization, Pharm Res. 2012;29:2939-2942.
8. Fürst R, Vollmar AM, A new perspective on old drugs: Non-mitotic actions of tubulin-binding drugs play a major role in cancer treatment, Die Pharmaz., 2013;68:478-483.
9. Prota AE, Bargsten K, Zurwerra D, Field JJ, Díaz JF, Altmann K-H, Steinmetz MO, Molecular Mechanism of Action of Microtubule-Stabilizing Anticancer Agents, Science. 2013;339:587-590.
10. Seligmann J, Twelves C, Tubulin: an example of targeted chemotherapy, Fut. Med. Chem. 2013;5:339-352.
11. Yamazaki Y, Tanaka K, Nicholson B, Deyanat-Yazdi G, Potts B, Yoshida T, Oda A, Kitagawa T, Orikasa S, Kiso Y, Yasui H, Akamatsu M, Chinen T, Usui T, Shinozaki Y, Yakushiji F, Miller BR, Neuteboom S, Palladino M, Kanoh K, Lloyd GK, Hayashi Y, Synthesis and Structure–Activity Relationship Study of Antimicrotubule Agents Phenylahistin Derivatives with a Didehydropiperazine-2,5-dione Structure, J. Med. Chem. 2011;55:1056-1071.
12. Abdel-Aziz M, Aly OM, Khan SS, Mukherjee K, Bane S, Synthesis, Cytotoxic Properties and Tubulin Polymerization Inhibitory Activity of Novel 2-Pyrazoline Derivatives, Arch. Parmaz. 2012;345:535-548.
13. Cao R, Liu M, Yin M, Liu Q, Wang Y, Huang N, Discovery of Novel Tubulin Inhibitors via Structure-Based Hierarchical Virtual Screening, J. Chem. Inf. Mod. 2012;52:2730-2740.
14. Chakraborti S, Chakravarty D, Gupta S, Chatterji BP, Dhar G, Poddar A, Panda D, Chakrabarti P, Ghosh Dastidar S, Bhattacharyya B, Discrimination of Ligands with Different Flexibilities Resulting from the Plasticity of the Binding Site in Tubulin, Biochem. 2012;51:7138-7148.
15. Chen J, Ahn S, Wang J, Lu Y, Dalton JT, Miller DD, Li W, Discovery of Novel 2-Aryl-4-benzoyl-imidazole (ABI-III) Analogues Targeting Tubulin Polymerization As Antiproliferative Agents, J. Med. Chem. 2012;55:7285-7289.
16. Coderch C, Morreale A, Gago F, Tubulin-based Structure-affinity Relationships for Antimitotic Vinca Alkaloids, Anti- Cancer Ag. Med. Chem., 2012;12:219-225.
17. Hidaka M, Koga T, Kiyota H, Horiguchi T, Shi Q-W, Hirose K, Uchida T, Relationship between the Structures of Taxane Derivatives and Their Microtubule Polymerization Activity, Biosci., Biotech. Biochem. 2012;76:349-352.
18. Hu L, Song W, Meng Y, Guo D, Liu X, Hu L, Synthesis and structure–activity relationship studies of cytotoxic vinorelbine amide analogues, Bioorg. Med. Chem. Let. 2012;22:7547-7550.

19. Leggans EK, Duncan KK, Barker TJ, Schleicher KD, Boger DL, A Remarkable Series of Vinblastine Analogues Displaying Enhanced Activity and an Unprecedented Tubulin Binding Steric Tolerance: C20′ Urea Derivatives, J. Med. Chem. 2012;56:628-639.
20. Rani P, Kainsa S, Kumar P, Medicinal Plants of Asian Origin having Anticancer Potential: Short Review, Asian J. Biomed. Pharm. Res. 2012;2:1-7.
21. Reddy MVR, Akula B, Cosenza SC, Lee CM, Mallireddigari MR, Pallela VR, Subbaiah DRCV, Udofa A, Reddy EP, (Z)-1-Aryl-3-arylamino-2-propen-1-ones, Highly Active Stimulators of Tubulin Polymerization: Synthesis, Structure–Activity Relationship (SAR), Tubulin Polymerization, and Cell Growth Inhibition Studies, J. Med. Chem. 2012;55:5174-5187.
22. Stec-Martyna E, Ponassi M, Miele M, Parodi S, Felli L, Rosano C, Structural Comparison of the Interaction of Tubulin with Various Ligands Affecting Microtubule Dynamics, Curr. Cancer Drug Tar. 2012;12:658-666.
23. Wang Z, Chen J, Wang J, Ahn S, Li C-M, Lu Y, Loveless V, Dalton J, Miller D, Li W, Novel Tubulin Polymerization Inhibitors Overcome Multidrug Resistance and Reduce Melanoma Lung Metastasis, Pharm Res. 2012;29:3040-3052.
24. Yamazaki Y, Sumikura M, Masuda Y, Hayashi Y, Yasui H, Kiso Y, Chinen T, Usui T, Yakushiji F, Potts B, Neuteboom S, Palladino M, Lloyd GK, Hayashi Y, Synthesis and structure–activity relationships of benzophenone-bearing diketopiperazine-type anti-microtubule agents, Bioorg. Med. Chem. 2012;20:4279-4289.
25. Assadieskandar A, Amini M, Ostad SN, Riazi GH, Cheraghi-Shavi T, Shafiei B, Shafiee A, Design, synthesis, cytotoxic evaluation and tubulin inhibitory activity of 4-aryl-5-(3,4,5-trimethoxyphenyl)-2-alkylthio-1H-imidazole derivatives, Bioorg. Med. Chem. 2013;21:2703-2709.
26. Gangjee A, Zhao Y, Raghavan S, Rohena CC, Mooberry SL, Hamel E, Structure–Activity Relationship and *In Vitro* and in Vivo Evaluation of the Potent Cytotoxic Anti-microtubule Agent N-(4-Methoxyphenyl)-N,2,6-trimethyl-6,7-dihydro-5H-cyclopenta [d] pyrimidin-4-aminium Chloride and Its Analogues As Antitumor Agents, J. Med. Chem. 2013;56:6829-6844.
27. Mangla V, Nepali K, Singh G, Singh J, Guru S, Gupta MK, Mahajan P, Saxena AK, Dhar KL, Structure Activity Relationship of Arylidene Pyrrolo and Pyrido [2,1-b] Quinazolones as Cytotoxic Agents: Synthesis, SAR Studies, Biological Evaluation and Docking Studies, Med. Chem. 2013;9:642-650.
28. Xi J, Zhu X, Feng Y, Huang N, Luo G, Mao Y, Han X, Tian W, Wang G, Han X, Luo R, Huang Z, An J, A novel class of tubulin inhibitors with promising anticancer activities, Mol. Cancer Res. 2013;11:856-864.
29. Bauer A, Bronstrup M, Industrial natural product chemistry for drug discovery and development, Nat. Prod. Rep. 2014;31:35-60.
30. Orlikova B, Legrand N, Panning J, Dicato M, Diederich M, "Anti-Inflammatory and Anticancer Drugs from Nature," in Advances in Nutrition and Cancer, V. Zappia, S. Panico, G. L. Russo, A. Budillon, and F. Della Ragione Eds.., Springer Berlin Heidelberg. 2014;159123-143.
31. Agin D, Hersh L, Holtzman D, The action of anesthetics on excitable membranes: a quantum-chemical analysis, Proc. Natl. Acad. Sci. (USA). 1965;53:952-958.
32. Cammarata A, An Apparent Correlation between the *In Vitro* Activity of Chloramphenicol Analogs and Electronic Polarizability, J. Med. Chem., 1967;10:525-527.
33. Cammarata A, Stein RL, Molecular orbital methods in the study of cholinesterase inhibitors, J. Med. Chem. 1968;11:829-833.
34. Cammarata A, Yau SJ, Predictability of correlations between *In vitro* tetracycline potencies and substituent indices, J. Med. Chem. 1970;13:93-97.

35. Peradejordi F, Martin AN, Cammarata A, Quantum chemical approach to structure-activity relationships of tetracycline antibiotics, J. Pharm. Sci. 1971;60:576-582.
36. Gómez Jeria JS, La Pharmacologie Quantique, Boll. Chim. Farmac. 1982;121:619-625.
37. Gómez-Jeria JS, On some problems in quantum pharmacology I. The partition functions, Int. J. Quant. Chem. 1983;23:1969-1972.
38. Gómez-Jeria JS, "Modeling the Drug-Receptor Interaction in Quantum Pharmacology," in Molecules in Physics, Chemistry, and Biology, J. Maruani Ed., Springer Netherlands. 1989;4:215-231,
39. Gómez-Jeria JS, Ojeda-Vergara M, Donoso-Espinoza C, Quantum-chemical Structure-Activity Relationships in carbamate insecticides, Mol. Engn. 1995;5:391-401.
40. Gómez-Jeria JS, Ojeda-Vergara M, Parametrization of the orientational effects in the drug-receptor interaction, J. Chil. Chem. Soc. 2003;48:119-124.
41. Gómez-Jeria JS, Elements of Molecular Electronic Pharmacology (in Spanish), Ediciones Sokar, Santiago de Chile; 2013.
42. Gómez-Jeria JS, A New Set of Local Reactivity Indices within the Hartree-Fock-Roothaan and Density Functional Theory Frameworks, Canad. Chem. Trans. 2013;1:25-55.
43. Tomas F, Aulló JM, Monoamine oxidase inhibition by β-carbolines: A quantum chemical approach, J. Pharm. Sci. 1979;68:772-776.
44. Hudson RF, Klopman G, A general perturbation treatment of chemical reactivity, Tet. Lett. 1967;8:1103-1108.
45. Klopman G, Hudson RF, Polyelectronic perturbation treatment of chemical reactivity, Theoret. Chim. Acta. 1967;8:165-174.
46. Fukui K, Fujimoto H, Frontier orbitals and reaction paths*:* selected papers of Kenichi Fukui*,* World Scientific, Singapore; River Edge, N.J.; 1997.
47. Gómez-Jeria JS, Morales-Lagos D, "The mode of binding of phenylalkylamines to the Serotonergic Receptor," in QSAR in design of Bioactive Drugs, M. Kuchar Ed., Prous, Barcelona JR, Spain. 1984;145-173.
48. Gómez-Jeria JS, Morales-Lagos DR, Quantum chemical approach to the relationship between molecular structure and serotonin receptor binding affinity, J. Pharm. Sci. 1984;73:1725-1728.
49. Gómez-Jeria JS, Morales-Lagos D, Rodriguez-Gatica JI, Saavedra-Aguilar JC, Quantum-chemical study of the relation between electronic structure and pA2 in a series of 5-substituted tryptamines, Int. J. Quant. Chem. 1985;28:421-428.
50. Gómez-Jeria JS, Morales-Lagos D, Cassels BK, Saavedra-Aguilar JC, Electronic structure and serotonin receptor binding affinity of 7-substituted tryptamines QSAR of 7-substituted tryptamines, Quant. Struct.-Relat. 1986;5:153-157.
51. Gómez-Jeria JS, Sotomayor P, Quantum chemical study of electronic structure and receptor binding in opiates, J. Mol. Struct. (Theochem). 1988;166:493-498.
52. Gómez-Jeria JS, Ojeda-Vergara M, Electrostatic medium effects and formal quantum structure-activity relationships in apomorphines interacting with D1 and D2 dopamine receptors, Int. J. Quant. Chem. 1997;61:997-1002.
53. Gómez-Jeria JS, Lagos-Arancibia L, Quantum-chemical structure-affinity studies on kynurenic acid derivatives as Gly/NMDA receptor ligands, Int. J. Quant. Chem. 1999;71:505-511.
54. Gómez-Jeria JS, Lagos-Arancibia L, Sobarzo-Sánchez E, Theoretical study of the opioid receptor selectivity of some 7-arylidenenaltrexones, Bol. Soc. Chil. Quím. 2003;48:61-66.
55. Gómez-Jeria JS, Soto-Morales F, Larenas-Gutierrez G, A Zindo/1 Study of the Cannabinoid-Mediated Inhibition of Adenylyl Cyclase, Ir. Int. J. Sci. 2003;4:151-164.

56. Gómez-Jeria JS, Gerli-Candia LA, Hurtado SM, A structure-affinity study of the opioid binding of some 3-substituted morphinans, J. Chil. Chem. Soc. 2004;49:307-312.
57. Soto-Morales F, Gómez-Jeria JS, A theoretical study of the inhibition of wild-type and drug-resistant HTV-1 reverse transcriptase by some thiazolidenebenzenesulfonamide derivatives, J. Chil. Chem. Soc. 2007;52:1214-1219.
58. Gómez-Jeria JS, Soto-Morales F, Rivas J, Sotomayor A, A theoretical structure-affinity relationship study of some cannabinoid derivatives, J. Chil. Chem. Soc. 2008;53:1393-1399.
59. Gómez-Jeria JS, A DFT study of the relationships between electronic structure and peripheral benzodiazepine receptor affinity in a group of N,N-dialkyl-2- phenylindol-3-ylglyoxylamides (Erratum in: J. Chil. Chem. Soc., 55, 4, IX, 2010), J. Chil. Chem. Soc. 2010;55:381-384.
60. Bruna-Larenas T, Gómez-Jeria JS, A DFT and Semiempirical Model-Based Study of Opioid Receptor Affinity and Selectivity in a Group of Molecules with a Morphine Structural Core, Int. J. Med. Chem. 2012;1-16. 2012 Article ID 682495.
61. Salgado-Valdés F, Gómez-Jeria JS, A theoretical study of the relationships between electronic structure and CB1 and CB2 cannabinoid receptor binding affinity in a group of 1-aryl-5-(1-H-pyrrol-1-yl)-1-H-pyrazole- 3-carboxamides., J. Quant. Chem. 2014;Article ID 431432:1-15.
62. Rogers KS, Cammarata A, A molecular orbital description of the partitioning of aromatic compounds between polar and nonpolar phases, Biochem. Biophys. Acta-Biomembr. 1969;193:22-29.
63. Rogers KS, Cammarata A, Superdelocalizability and charge density. A correlation with partition coefficients, J. Med. Chem. 1969;12:692-693.
64. Cammarata A, Rogers KS, Electronic representation of the lipophilic parameter π, J. Med. Chem. 1971;14:269-274.
65. Barahona-Urbina C, Nuñez-Gonzalez S, Gómez-Jeria JS, Model-based quantum-chemical study of the uptake of some polychlorinated pollutant compounds by Zucchini subspecies, J. Chil. Chem. Soc. 2012;57:1497-1503.
66. Gómez-Jeria JS, Flores-Catalán M, Quantum-chemical modeling of the relationships between molecular structure and *In vitro* multi-step, multimechanistic drug effects. HIV-1 replication inhibition and inhibition of cell proliferation as examples., Canad. Chem. Trans. 2013;1:215-237.
67. Paz de la Vega A, Alarcón DA, Gómez-Jeria JS, Quantum Chemical Study of the Relationships between Electronic Structure and Pharmacokinetic Profile, Inhibitory Strength toward Hepatitis C virus NS5B Polymerase and HCV replicons of indole-based compounds., J. Chil. Chem. Soc. 2013;58:1842-1851.
68. Stone KR, Mickey DD, Wunderli H, Mickey GH, Paulson DF, Isolation of a human prostate carcinoma cell line (DU 145), Int. J. Cancer. 1978;21:274-281.
69. Lozzio C, Lozzio B, Human chronic myelogenous leukemia cell-line with positive Philadelphia chromosome, Blood. 1975;45:321-334.
70. Drexler HG, The leukemia-lymphoma cell line factsbook. Academic Press, San Diego, CA; 2000.
71. Frisch MJ, Trucks GW, Schlegel HB et al. Gaussian98 Rev. A.11.3, Gaussian, Pittsburgh, PA, USA; 2002.
72. Gómez-Jeria JS, An empirical way to correct some drawbacks of Mulliken Population Analysis (Erratum in: J. Chil. Chem. Soc., 55, 4, IX, 2010), J. Chil. Chem. Soc. 2009;54:482-485.
73. Statsoft, Statistica 8.0, 2300 East 14 th St. Tulsa, OK 74104, USA; 1984-2007.

74. Gómez-Jeria JS, Approximate Molecular Electrostatric Potentials of Protonated Mescaline Analogues, Acta sud Amer. Quím.1984;4:1-9.



*Peer-review history:*
*The peer review history for this paper can be accessed here:*
*http://www.sciencedomain.org/review-history.php?iid=475&id=16&aid=4195*